

**Bacterial Acidity-Triggered Antimicrobial Activity of Self-assembling Peptide Nanofibers**

| | |
|-------------------------------|---|
| Journal: | <i>Journal of Materials Chemistry B</i> |
| Manuscript ID | TB-COM-01-2019-000134.R1 |
| Article Type: | Communication |
| Date Submitted by the Author: | 27-Mar-2019 |
| Complete List of Authors: | CHEN, WEIKE; University of Texas at Arlington, Chemistry and Biochemistry Li, Shuxin; University of Texas at Arlington, Bioengineering Renick, Paul; University of Texas at Arlington, Biology Yang, Su; University of Texas at Arlington Pandey, Nikhil; University of Texas at Arlington, Bioengineering Boutte, Cara; University of Texas at Arlington, Biology Nguyen, Kytai T. ; University of Texas at Arlington, Bioengineering Tang, Liping; The University of Texas at Arlington, Bioengineering; Dong, He; University of Texas at Arlington, Chemistry and Biochemistry |
| | |



Journal Name

COMMUNICATION

Bacterial Acidity-Triggered Antimicrobial Activity of Self-assembling Peptide Nanofibers

Weike Chen,^a Shuxin Li,^b Paul Renick,^c Su Yang,^a Nikhil Pandey,^b Cara Boutte,^c Kytai T. Nguyen,^b Liping Tang,^{*,b} and He Dong^{*,a}

Received 00th January 20xx,
Accepted 00th January 20xx

DOI: 10.1039/x0xx00000x

www.rsc.org/

A self-assembling peptide nanofiber is developed to sense the microenvironmental pH change associated with bacterial growth. Using a near-infrared probe, a strong correlation was observed between the local pH reduction of bacterial colonies with the degree of peptide disassembly, which led to their enhanced antimicrobial activity against anaerobic bacteria.

Trigger-responsive nanomaterials have tremendous promise for targeted therapeutic delivery strategies that improve the treatment of a variety of diseases.¹ Among various approaches, self-assembly has been proven as an effective bottom-up approach to construct functional nanomaterials. A wide range of molecular building blocks, including amphiphilic polymers, lipids, proteins and peptides can be custom-designed and assembled into “smart” nanomaterials that can sense various disease-specific microenvironmental conditions.² Self-assembled nanomaterials can easily change their physicochemical properties in response to the environmental change and lead to local release of therapeutics with enhanced drug potency and reduced side effects on healthy tissues and cells. In recent years, great levels of success have been achieved for nanomaterials designed for targeted cancer therapy.³ However, the development of self-assembled nanomaterials for targeted antimicrobial delivery is just getting underway for infectious disease treatment.⁴

Similar to some of the tumor tissues, certain bacteria can reduce the local pH of the infection tissues through low oxygen triggered anaerobic fermentation.⁵ Host immune response can further lower the local pH where bacteria reside through mechanisms of production of lactic acids during phagocytosis.⁶ While the acidic pH is considered as an undesirable factor causing the reduction of the antimicrobial activity of several classes of antibiotics,⁷ it can be utilized as a natural physiological cue for the design of antimicrobial

nanomaterials for targeted antimicrobial delivery. Recent reports have demonstrated advances in the design of acid-sensitive nanoparticles for targeting the bacterial membrane and delivery of small molecule antibiotics to treat bacterial infections in acidic conditions.^{4a} Acid-dependent helical polypeptides were also reported to selectively target and eradicate pathogenic *H. pylori* without affecting commensal bacteria in the stomach.^{4d} These successful examples provide the inspiration and highlight the feasibility of using pH as a physiological trigger to achieve targeted antimicrobial therapy.

In this work, we sought to develop a novel acid-activatable antimicrobial therapy by capitalizing on our recent development of self-assembling nanofibers (SANs) for bacterial acidity triggered antimicrobial delivery. SANs are supramolecular assemblies of *de novo* designed multidomain peptides (MDPs) that have been explored as highly cytocompatible antimicrobial and cell penetrating nanomaterials.⁸ The first generation of MDPs has a general formula of $K_x(QL)_yK_z$ (amino acid single code letter K: Lysine, Q: Glutamine, L: Leucine) to mimic natural cationic antimicrobial peptides (AMPs). Unlike most conventional AMPs that exist as monomers in solution, MDPs can form supramolecular β -sheet nanofibers in which the hydrophobic residues and non-polar surface are partially masked between the two sheets, which has been proven as an important factor to minimize the cytotoxicity of MDPs toward mammalian cells.⁹ The cytocompatibility of SANs was greatly enhanced compared to that of traditional monomeric AMPs. However, the confinement of the hydrophobic moiety within the assembly can also reduce their antimicrobial activity while monomeric AMPs are more potent to kill bacteria. As such, the current study by developing SANs that undergo pH-responsive disassembly combines the advantages of both self-assembled peptides in terms of their cytocompatibility and monomeric AMPs in terms of their antimicrobial activity to treat acidity-associated bacterial infection. The central hypothesis is SANs under the physiological condition are bio-inert because the membrane-interacting hydrophobic moieties of SANs are buried inside the assembly and not accessible to the cell membrane. At the bacterial colonization site with an acidic pH, MDPs become charged and the increased charge density triggers SANs disassembly and

^a Department of Chemistry and Biochemistry, The University of Texas at Arlington, Arlington, TX, 76019, USA. Email: he.dong@uta.edu.

^b Department of Bioengineering, The University of Texas at Arlington, Arlington, TX, 76019, USA.

^c Department of Biology, The University of Texas at Arlington, Arlington, TX, 76019, USA.

†Electronic Supplementary Information (ESI) available: Materials, experimental procedures and supplementary figures. See DOI: 10.1039/x0xx00000x

subsequent release of activated peptides to effectively interact with the cell membrane and kill bacteria (**Figure 1**).

Three MDPs with the sequences of $\text{WH}_5(\text{QL})_6\text{K}_2$, $\text{WH}_7(\text{QL})_6\text{K}_2$, and $\text{WH}_9(\text{QL})_6\text{K}_2$ abbreviated as WH_5 , WH_7 and WH_9 (H: Histidine, W: Tryptophan) were initially explored as the building units to fabricate SANs. The sequences were chosen based on the following considerations. First, the central repeating (QL) domain provides the driving force for SANs formation under the neutral physiological condition as discussed in our previous studies.^{8b} Second, oligo-histidine of different lengths was incorporated at the N-terminus to endow pH-responsiveness to SANs. At a pH below the pKa of histidine, peptides become charged. The electrostatic repulsion among the positively charged MDPs will destabilize SANs and lead to the release of activated MDPs that can effectively eradicate bacteria. Third, the numbers of histidine residues are varied in order to integrate and achieve a good balance between self-assembly under the neutral condition and disassembly upon acidification. MDPs with different numbers of histidine would render a small library to explore the effect of charge on SANs stability, disassembly efficiency and their resulting biological activities. Lastly, two lysine residues were appended at the C-terminus to ensure sufficient solubility of SANs and minimize lateral fiber aggregation through electrostatic repulsion. All peptides contain a tryptophan residue for accurate determination of the peptide concentration by UV spectroscopy.

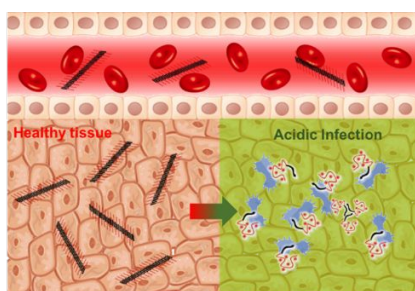


Figure 1. Cartoon representation of cytocompatible and hemocompatible SANs formed by pH-responsive MDPs and their disassembly triggered by local bacterial acidity for the delivery of activated MDPs to eradicate bacteria.

Elucidating the physicochemical properties of MDPs as a function of pH is critical to tailoring their biological activities. Critical assembly concentration (CAC) measurements were first conducted to investigate their ability to assemble under different pH conditions. As shown in **Figure S2**, a non-linear relationship was observed for all three MDPs at pH 7.4 (Tris buffer, 20 mM) suggesting the formation of higher ordered assemblies as the concentration increased. At an acidic pH (MES buffer, pH 5.7, 20 mM), a linear correlation was found between the fluorescence intensity and peptide concentrations, suggesting the majority of peptides do not self-assemble and rather remain isolated. It is worth noting that we chose pH 5.7 as the acidic condition for this study in order to achieve a good balance between the protonation degree of histidine ($\text{pK}_a \sim 6$) and bacterial growth under the acidic condition. The pH-dependent self-assembly and disassembly was further investigated and confirmed by circular dichroism (CD) spectroscopy. At pH 7.4, all three peptides exhibited predominant β -sheet structures as characterized by a minimum peak between 210-220 nm (**Figure S3a**) indicating the formation of SANs. When the pH is reduced to 5.7, which is below the pKa point of histidine, the presumed increase in positive charges and electrostatic repulsion triggered disassembly and unfolding of β -sheets to random

coils and/or weak helices. As shown in **Figure S3b**, all three MDPs unfolded upon pH reduction, but to different degrees. WH_7 and WH_9 exhibited more disordered structures than WH_5 given the larger blue shifts of the minimum absorption down to ~ 203 nm indicating a greater tendency to disassemble. To quantitatively determine the extent of SANs disassembly, spin dialysis was used to estimate the amounts of disassembled MDPs upon pH reduction. Centrifugal filters with molecular weight (MW) cutoff at 10 kDa and 30 kDa were used to separate the monomeric MDP and any potential non-specific aggregates (up to 9 mers) (due to their amphiphilic nature) from the residual higher ordered assemblies, respectively. As shown in **Table 1**, no materials were detected in the filtrate for all three MDPs through spin dialysis suggesting the stability and integrity of SANs at the neutral pH. At the acidic pH, disassembly occurs as shown by the increased concentrations of MDPs in the filtrate using both filters. It was estimated that 24.60% of WH_5 , 34.70% of WH_7 and 41.00% of WH_9 were disassembled to monomers based on the dialysis result using the filter with a MW cutoff at 10 kDa. Using a 30 kDa filter, the percentage of MDPs in the filtrate increased to 37.77%, 62.56% and 71.46% for WH_5 , WH_7 and WH_9 , respectively.

Table 1. Quantification of disassembled MDPs

| Peptides | 10 kDa filter | | 30 kDa filter | |
|---------------|---------------|--------------------|---------------|--------------------|
| | pH 7.4 | pH 5.7 | pH 7.4 | pH 5.7 |
| WH_5 | 0 | $24.60 \pm 0.08\%$ | 0 | $37.77 \pm 0.56\%$ |
| WH_7 | 0 | $34.70 \pm 0.08\%$ | 0 | $62.56 \pm 3.55\%$ |
| WH_9 | 0 | $41.00 \pm 0.49\%$ | 0 | $71.64 \pm 0.27\%$ |

Standard deviation is calculated based on 3 measurements for each sample

The filtrate of WH_9 at pH 5.7 was analyzed by CD spectroscopy showing highly disordered random coil structures (**Figure S3c**), thus excluding the possibility of the presence of β -sheet oligomers in the filtrate. The oligomeric species present in the filtrate is likely due to the non-specific aggregation between the amphiphilic MDPs. Transmission electron microscopy (TEM) reveals the morphological change of MDPs under different pH treatments. For TEM characterization and the following biological evaluation, we primarily focused on WH_9 because it is the most sensitive to pH change giving a higher extent of disassembly upon solution acidification. At pH 7.4, WH_9 spontaneously self-assembled to form elongated fibers (**Figure 2a**). Reducing the pH to 5.7 led to a significant reduction of the fiber density and the formation of non-specific spherical aggregates (**Figure 2b**). We suspect that these spherical aggregates were formed from disassembled MDPs due to the drying effect during TEM sample preparation process. The disassembly of SANs was verified by dynamic light scattering (DLS) measurements showing a dramatically reduced particle size to below 2 nm when pH was reduced (**Figure 2c** and **Figure S4**). Although the number mean of the hydrodynamic diameter generated by DLS does not represent the actual size of these nanofibers due to their non-spherical shapes, the dramatic size reduction suggests the effectiveness of solution acidity to trigger the disassembly of SANs.

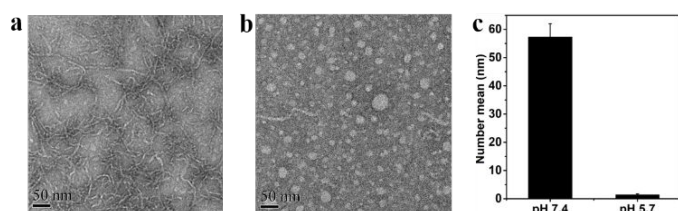


Figure 2. Negatively stained TEM images of WH₉ at (a) pH 7.4 showing SANs formation and (b) at pH 5.7 showing SANs disassembly. (c) pH-dependent hydrodynamic size measurement by DLS. Peptide concentration: 100 μ M in Tris buffer (pH 7.4, 20 mM) and MES buffer (pH 5.7, 20 mM)

Acidity-triggered SANs disassembly was further studied in the context of bacterial inoculation on an agar plate. We chose *Bacteroides fragilis* as a model bacterium that undergoes anaerobic growth leading to the acidification of the surrounding environment. We first determined whether the growth of *B. fragilis* would influence the pH immediately adjacent to the bacterial colony. Using a pH ratiometric near infrared probe developed recently,¹⁰ we measured the change of fluorescent intensity of the probe with time using an *in vivo* Kodak imager. The results allow us to calculate the pH nearby the colony on an agar plate at 0.5, 2.5, 7, and 22.5 hrs upon bacterial inoculation. Interestingly, we find that growth of *B. fragilis* releases metabolites which can cause the surrounding environment to become acidic (from pH 7.5 to pH 6.3 in less than 24 hrs) (Figure S5). To test whether the in-situ low pH can induce SANs disassembly, we synthesized and prepared rhodamine (Rho)-labeled WH₉. Rho-WH₉ has very low fluorescent intensity due to fluorescent quenching upon self-assembly. By reducing the local pH, WH₉ disassembles leading to the recovery of rhodamine fluorescence. Therefore the fluorescence intensity of the peptide reflects the degree of peptide disassembly and can be used to correlate with the microenvironmental pH change associated with bacterial growth. To determine whether the acidic environment nearby bacterial colonies causes SANs to disassemble, Rho-WH₉ was applied on both the bacterial colonies and non-inoculated agars as controls after 24 hrs of bacterial inoculation. The fluorescence intensity was monitored immediately using an *in vivo* Kodak imager. The results showed an average of 88% increase of the fluorescence intensity for peptides deposited on the bacteria colonies than those on the agar media without bacteria (Figure 3a), suggesting a local acidic pH can trigger the disassembly of SANs, leading to the recovery of self-quenched fluorescence. The fluorescence intensity of the peptide across the bacterial colony was further plotted as a function of imaging pixels (~0.1 mm/per pixel) starting from the outermost of a colony (shown as 0 on the x-axis of Figure 3b) while moving toward the center (shown as 10 on the x-axis of Figure 3b). The local bacterial pH change across a single colony was measured by the ratiometric fluorescence probe described above and plotted in the same manner. A good correlation was observed between the reduced pH and the increased fluorescence of Rho-WH₉, further confirming local bacterial acidity can trigger SANs disassembly.

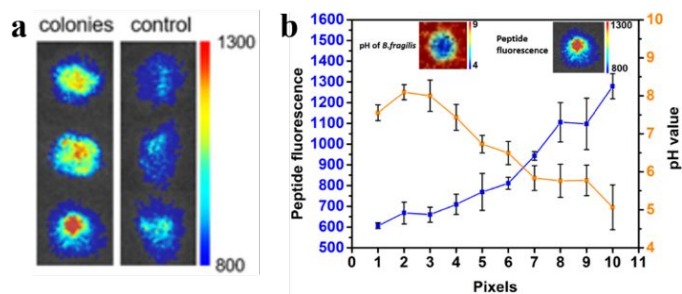


Figure 3. Local bacterial acidity triggered peptide disassembly as determined by in situ fluorescence microscopy. a) Fluorescence intensity of Rho-labeled WH₉ deposited on 3 bacterial colonies (3 spots on the left panel) compared to those on agar media (right panel) without bacteria showing that the acidic bacterial environment can induce SANs disassembly that led to a recovery of the self-quenched rhodamine fluorescence. b) Correlation of the local bacterial pH (orange line) with the fluorescence intensity of Rho-labeled WH₉ (blue lines) applied on bacterial colonies. The inset pictures are fluorescent microscopic images of bacterial colonies upon Rho-labeled peptide treatment (right) and colonies containing the near infrared pH probe (left).

The antimicrobial activities of WH₉ were tested against both gram-negative bacteria, *Escherichia coli* and *B. fragilis* and gram-positive bacteria, *Staphylococcus aureus* under the anaerobic condition where bacterial cultures became acidic over time. Peptides were co-incubated with *E. coli*, *B. fragilis* and *S. aureus* for 48 hrs and the UV absorbance at 600 nm was measured for the estimation of the minimum inhibitory concentration (MIC) values. As shown in Table 2, WH₉ was effective against all three bacterial strains in the anaerobic condition where the bacterial culture gradually became acidic to pH 6.4. The MIC values of WH₉ were determined at 10 μ M against *E. coli*, 5 μ M against *B. fragilis* and 5 μ M against *S. aureus*. In contrast, the MIC of WH₉ was estimated at 40 μ M against *E. coli* in the aerobic condition where the culture pH remained neutral (pH was between 7.2 and 7.5 during culture). For aerobic bacterial cultures with a starting pH at 5.7, the MIC was determined as 10 μ M comparable to that determined in the anaerobic condition. In comparison, the MICs of WH₅ and WH₇ were determined at 40 μ M and 20 μ M in the acidic aerobic *E. coli* cultures showing less potency to inhibit the growth of bacteria. The antimicrobial activity also correlates well with the peptide's ability to disassemble as detailed in the spin dialysis experiment (Table 1).

Table 2. Antimicrobial activity, cytotoxicity and hemolytic activity

| | | | MIC (μ M) | | IC ₅₀ μ M | HC ₁₀ μ M |
|----------------|--------------------|------------------|----------------|--------|-----------------------------|-----------------------------|
| | | Anaerobic | Aerobic | | | |
| <i>E. coli</i> | <i>B. fragilis</i> | <i>S. aureus</i> | <i>E. coli</i> | | | |
| | | | pH 7.4 | pH 5.7 | | |
| 10 | 5 | 5 | > 40 | 10 | >80 | >160 |

The mode of antimicrobial action was investigated by epifluorescence microscopy. WH₉ was co-incubated with *E. coli* aerobically so that the culture pH can be adjusted and maintain at

either acidic or neutral during the entire culture. A live-dead assay was performed wherein *E. coli* was incubated with WH₉ for 3 hrs, followed by staining with SYTO9 and Propidium Iodide (PI). As shown in (Figure 4a), a much higher fraction of *E. coli* cells fluoresced red at the acidic pH due to pH-triggered disassembly and release of peptides that can increase the membrane permeability of PI. At the neutral pH (Figure 4b), the peptide was confined within the SANS and does not have sufficient freedom to access to and further permeate the bacterial cell membrane. The live-dead assay was also performed in Gram-positive *S. aureus* culture showing the same trend of pH-dependent antimicrobial activity (Figure S6).

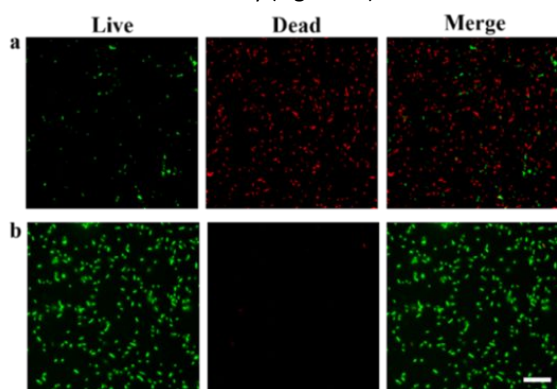


Figure 4. Fluorescence images of Live/dead bacterial assay results. Top panel: *E. coli* treated with 20 μM WH₉ at (a) pH 5.7 and (b) pH 7.4 for 3hrs. Live bacteria were stained with SYTO9 (green) and dead bacteria was stained with PI (red). Scale bar: 20 μm .

The physical interaction between WH₉ and bacteria was also studied by fluorescence microscopy upon incubation of FITC-labelled WH₉ with *E. coli* followed by PI staining. The binding affinity of WH₉ toward bacteria was greatly improved upon acidification as demonstrated by the numbers of bacterial cells that are attached by peptides showing green fluorescence on the cell membrane (Figure S7a) while at the neutral condition much less binding occurs between the peptides and bacteria (Figure S7b). Scan electron microscopy (SEM) was used to visualize any morphological change induced in bacteria by exposure to WH₉ at the acidic condition. As compared to control bacteria without peptide treatment (Figure S8a), *E. coli* incubated with WH₉ under the acidic culture condition showed significant membrane damage (Figure S8b), suggesting the mode of action is through bacterial membrane disruption by the disassembled peptides.

A critical challenge associated with conventional AMPs is their moderate to severe cytotoxicity and hemolytic activity.¹¹ We have recently demonstrated that self-assembly can be an effective approach to reduce the non-polar membrane-contact area of AMPs leading to greatly improved cytocompatibility and bacterial cell selectivity.⁹ To evaluate the cytotoxicity of the newly designed WH₉ toward mammalian cells during blood circulation, NIH/3T3 fibroblasts were incubated with peptides at various concentrations and the cell viability was quantified by the MTT assay. 80 μM was selected as the upper concentration threshold to avoid potential precipitate formation as the peptide concentration increases in the mammalian culture media. As shown in Figure S9, dose-dependent cell viability was measured showing > 80% of cell viability up to 40 μM and 72% cells were still alive upon incubation with peptides at 80 μM . The hemocompatibility was evaluated by incubating human red

blood cells (RBCs) with WH₉ at different concentrations for 1 hr and released haemoglobin was measured by UV spectroscopy (Figure S10). Within the tested peptide concentrations up to 160 μM (16 times of the MIC) less than 5% of hemolysis was observed with peptide-treated RBCs compared to the positive control group of RBCs treated with Triton-100. Taken together, the pH-triggered antimicrobial activity and excellent cytocompatibility and hemocompatibility of self-assembled WH₉ highlight their great potential as a new antimicrobial strategy to effectively treat bacterial infections associated with acidity.

In summary, we have demonstrated a new pH-responsive antimicrobial nanomaterial based on the self-assembly of *de novo* designed MDPs for acid-responsive antimicrobial delivery at the site of infection associated with bacterial acidity. The MDP can be designed to form stable nanofibrous structure in neutral pH with excellent cytocompatibility and hemocompatibility. The pH-triggered disassembly was demonstrated in both the aqueous solution and on a bacteria-inoculated agar plate and shown to be important factors for their antimicrobial activity. This new antimicrobial strategy while awaiting more extensive *in vitro* evaluation and *in vivo* studies holds great promise to treat bacterial infections in which acidity plays an important role in bacteria pathogenesis. For future studies, SANS based on custom-designed non-natural amino acids may offer diverse chemical functionality and broader pH-tunability to suit various clinical needs in the combat of infectious diseases.

This study was supported by the National Science Foundation (DMR 1824614) and the start-up funds from the University of Texas at Arlington.

Conflicts of interest

There are no conflicts to declare.

Notes and references

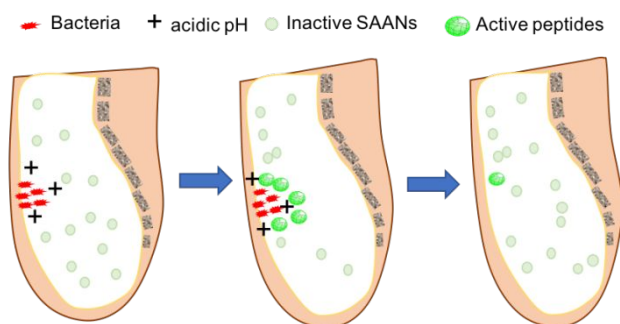
- (a) V. P. Torchilin, *Nat. Rev. Drug Discov.* 2014, **13**, 813; (b) O. Veisheh, B. C. Tang, K. A. Whitehead, D. G. Anderson and R. Langer, *Nat. Rev. Drug Discov.* 2014, **14**, 45; (c) E. J. Chung, L. B. Mlinar, K. Nord, M. J. Sugimoto, E. Wonder, F. J. Alenghat, Y. Fang and M. Tirrell, *Adv. Healthc. Mater.* 2015, **4**, 367; (d) L. L. Lock, Z. Tang, D. Keith, C. Reyes and H. Cui, *ACS Macro Lett.* 2015, **4**, 552; (e) Y. Wang and D. S. Kohane, *Nat. Rev. Mater.* 2017, **2**, 17020; (f) D. Rosenblum, N. Joshi, W. Tao, J. M. Karp and D. Peer, *Nat. Commun.* 2018, **9**, 1410.
- (a) H. J. Chung and T. G. Park, *Nano Today* 2009, **4**, 429; (b) H. Hosseinkhani, P.-D. Hong and D.-S. Yu, *Chem. Rev.* 2013, **113**, 4837; (c) L. Zhang, J. M. Chan, F. X. Gu, J.-W. Rhee, A. Z. Wang, A. F. Radovic-Moreno, F. Alexis, R. Langer and O. C. Farokhzad, *ACS Nano*. 2008, **2**, 1696.
- (a) L. Gu and D. J. Mooney, *Nat. Rev. Cancer*. 2015, **16**, 56; (b) D. A. Scheinberg, C. H. Villa, F. E. Escorcía and M. R. McDevitt, *Nat. Rev. Clin. Oncol.* 2010, **7**, 266; (c) J. A. Barreto, W. O'Malley, M. Kubeil, B. Graham, H. Stephan and L. Spiccia, *Adv. Mater.* 2011, **23**, H18; (d) Q. Sun, Z. Zhou, N. Qiu and Y. Shen, *Adv. Mater.* 2017, **29**, 1606628.
- (a) A. F. Radovic-Moreno, T. K. Lu, V. A. Puscasu, C. J. Yoon, R. Langer and O. C. Farokhzad, *ACS Nano*. 2012, **6**, 4279; (b) M. Hughes, S. Debnath, C. W. Knapp and R. V. Ulijn, *Biomater. Sci.*

- 2013, **1**, 1138; (c) B. Horev, M. I. Klein, G. Hwang, Y. Li, D. Kim, H. Koo and D. S. W. Benoit, *ACS Nano*. 2015, **9**, 2390; (d) M. Xiong, Y. Bao, X. Xu, H. Wang, Z. Han, Z. Wang, Y. Liu, S. Huang, Z. Song, J. Chen, R. M. Peek, L. Yin, L.-F. Chen and J. Cheng, *Proc. Natl. Acad. Sci. U.S.A.* 2017, **114**, 12675.
- 5 (a) S. Fuchs, J. Pané-Farré, C. Kohler, M. Hecker and S. Engelmann, *J. Bacteriol.* 2007, **189**, 4275; (b) B. Marteyn, F. B. Scorza, P. J. Sansonetti and C. Tang, *Cell. Microbiol.* 2011, **13**, 171.
- 6 (a) R. Dubos, *Lancet* 1955, **266**, xxiv; (b) A. S. Trevani, G. Andonegui, M. Giordano, D. H. López, R. Gamberale, F. Minucci and J. R. Geffner, *J. Immunol.* 1999, **162**, 4849; (c) B. J. Marsland and E. S. Gollwitzer, *Nat. Rev. Immunol.* 2014, **14**, 827; (d) M. Kilian, I. L. C. Chapple, M. Hannig, P. D. Marsh, V. Meuric, A. M. L. Pedersen, M. S. Tonetti, W. G. Wade and E. Zaura, *Bdj* 2016, **221**, 657.
- 7 R.-C. Mercier, C. Stumpo and M. J. Rybak, *J. Antimicrob. Chemother.* 2002, **50**, 19.
- 8 (a) D. Xu, D. Dustin, L. Jiang, D. S. K. Samways and H. Dong, *Chem. Commun.* 2015, **51**, 11757; (b) D. Xu, L. Jiang, A. Singh, D. Dustin, M. Yang, L. Liu, R. Lund, T. J. Sellati and H. Dong, *Chem. Commun.* 2015, **51**, 1289.
- 9 D. Xu, W. Chen, Y. J. Tobin-Miyaji, C. R. Sturge, S. Yang, B. Elmore, A. Singh, C. Pybus, D. E. Greenberg, T. J. Sellati, W. Qiang and H. Dong, *ACS Infect. Dis.* 2018, **4**, 1327.
- 10 Y.-T. Tsai, J. Zhou, H. Weng, J. Shen, L. Tang and W.-J. Hu, *Adv. Healthc. Mater.* 2014, **3**, 221.
- 11 W. Aoki, K. Kuroda and M. Ueda, *J. Biosci. Bioeng.* 2012, **114**, 365.

Graphical Abstract

Bacterial Acidity-Triggered Antimicrobial Activity of Self-assembling Peptide Nanofibers

Weike Chen, Shuxin Li, Paul Renick, Su Yang, Nikhil Pandey, Cara Boutte, Kytai T. Nguyen, Liping Tang*, He Dong*



A soluble, supramolecular peptide serves as an antimicrobial depot to release activated peptides in response to microenvironmental bacterial pH change.